ORIGINAL ARTICLE

Modeling the impact of land use changes on the trend of monthly temperature in Basrah province, Southern Iraq

Safaa A. R. Al-Asadi[1] · Tareq J. A. Almula[1] · Yaareb S. Abdulrazzaq[1] · Alaa M. Al-Abadi[2]

Abstract

The current study aims to analyze the trend of monthly average temperature in Basrah province to understand the role of land use changes in this pattern. Data which was recorded at Hay Al-Hussain station in the city of Basrah over a span of 74 years (1948–2022) were utilized for this purpose. The non-parametric Mann–Kendall test and Sen's slope estimator were used to estimate the trend and the magnitude of the trend, respectively. Findings revealed that the average temperature trend is increasing at a rate of 0.00475 °C/month (4.218 °C in total). This indicates that Basrah is experiencing a faster temperature increase than the global average (1 °C) and the Middle East region (2 °C). Five main factors contributed to the temperature rise in the study area: increasing oil fields, reduction of green cover, global warming, urban expansion, and wetland shrinkage. Furthermore, the study revealed that the impact of changes in land use outweighs the effect of global warming on the temperature rise in the study area. This finding could facilitate the implementation of measures to reduce the warming rate within Basrah and other regions inside and outside Iraq, for the purpose of adapting to the climate change effects that are already occurring. This can be achieved by controlling unplanned changes in land use and minimizing their negative effects on the increase of temperature.

Keywords Land use changes · Climate change · Temperature trend · Global warming · Environmental degradation

Introduction

Temperature is a key component that has a significant impact on both humans and environment. It influences many areas of life on Earth, from human health and well-being to ecosystem dynamics and climate patterns. Temperature exerts a profound influence on the behavior and spatial distribution of diverse species within ecosystems. It exerts a critical impact on the growth rates of plants, the metabolic rates of animals, and the intricate interactions among species (Parmesan and Yohe 2003). Alterations in temperature can result in significant modification in the composition of species, thereby impacting the delicate balance of predator–prey dynamics, interspecies competition, and the overall equilibrium of the ecosystem (Buckley et al. 2015). Temperature plays a pivotal role in climate patterns. It influences global atmospheric circulation, leading to the formation of weather systems, precipitation patterns, and wind currents (Roe and Steig 2004). Changing temperature contributes to shifting climate zones and more extreme weather events. Temperature changes can alter several hydrological processes, including precipitation and runoff patterns, which in turn also influence temperature (Tabari and Talaee 2011; Panda and Sahu 2019) Higher temperatures can aggravate drought conditions and increase water demand for agriculture, industry, and residential use, putting a strain on water resources.

Global warming is one of the most challenging environmental issues currently faced by the global community. This is due to human activity and the emissions of greenhouse gases (Farooq et al. 2021; Kotagama et al. 2023). Projected to rise in the average global surface temperature throughout

✉ Safaa A. R. Al-Asadi
  safaa.al_asadi@uobasrah.edu.iq

  Tareq J. A. Almula
  taraq.ali@uobasrah.edu.iq

  Yaareb S. Abdulrazzaq
  Yaroob81salman@gmail.com

  Alaa M. Al-Abadi
  alaa.atiaa@uobasrah.edu.iq

[1] Department of Geography, College of Education, University of Basrah, Basra, Iraq

[2] Department of Geography, College of Science, University of Basrah, Basra, Iraq

the twenty-first century by around 1.4–2.0 °C (Malik et al. 2022). The Middle East represents one of the region's most vulnerable to the impacts of climate change, due to the presence of arid and semi-arid areas. It is expected that countries in this region will experience an increase in temperature of more than 4.0 °C by the end of the twenty-first century (Osman-Elasha 2010; Mansouri Daneshvar et al. 2019). Iraq has been classified as one of the most five countries most vulnerable to climate change, due to the increasing impacts of greenhouse gas emissions over time as a result of the rise in crude oil production. It is expected that the temperature will increase by about 5.0 °C by the end of the twenty-first century (Hashim et al. 2022; Hassan et al. 2023).

Land use changes is one among the responsible factors for global warming (Jain et al. 2014; Halder et al. 2016), because of its direct role in changing surface physical properties such as surface reflectivity, surface roughness, and vegetation coverage (Hua et al. 2015; Li et al. 2017; Ru et al. 2022).

The province of Basrah has been subjected to the severest cases of climate change, manifested by a sharp rise in temperatures and accompanying drought conditions, which have affected economic activities and ecological systems. This has put pressure on the local and central governments. Unfortunately, awareness, by decision makers of the deteriorating climatic conditions in the region is inadequate, because they believing that this problem has global causes rather than local ones. This contributes to the increase of the rate of temperature rise, which could lead to a serious environmental disaster that may endanger the future of the population and their stability in the region. For instance, the decrease in the flow of freshwater in Basrah province during the summer of 2018 led to its contamination due to the sharp rise in temperatures. This resulted in the infection and toxicity of more than 118 individuals (Wille 2019).

There are numerous studies that have addressed the topic of climate change and its effect on health and the environment in the study region. They include both Iran and Saudi Arabia (Tarawneh and Chowdhury 2018; Mansouri Daneshvar et al. 2019; Mousavi et al. 2020; Odnoletkova et al. 2020). These studies collectively agree that temperatures are rising over time, and they identify the increase in carbon dioxide emissions from the energy sector and urbanization as the primary cause of this temperature increase.

The objectives of the current study are: (1) to determine the trends in monthly temperature averages in the province of Basrah; (2) to investigate the role of land use changes in the trend of temperature; and (3) an attempt to identify the primary potential causes of climate change, and seeking to assess the extent of each factor's impact on temperatures. This was done by using station-based data, remotely sensed data, and global hydrological models' data. This knowledge lays the foundation for devising sustainable management strategies and crafting effective mitigation plans for the province's climate-related challenges.

Material and methods

The study area

Basrah province is located in the southern part of Iraq, between 29°6′–31°16′N and 46°43′–48°37′E. It is bordered by Kuwait and the Kingdom of Saudi Arabia to the south, and Iran to the east. It shares local boundaries with Thi Qar and Maysan provinces to the north, and Muthanna provinces to the west (Fig. 1). Geomorphologically, the area of Basrah encompasses about 19,070 km², representing 4.4% of the total area of Iraq. The territory of the province can be categorized into two distinct physiographic regions: the Mesopotamian plain (which covers 44.6%) in the eastern part, and the Western Plateau (which covers 55.4%) in the west. Shatt Al-Basrah Canal separates these two sections. Except for Sanam hill (Jabal Sanam) near the Iraq-Kuwait border, the majority of the study region is flat and featureless. It has elevation ranges between 0 and 5 m at the plain and 5–250 m at the plateau.

Basrah province encompasses numerous bodies and water resources, as it includes the Tigris and Euphrates rivers that confluence in the northern part. The twin rivers form the Shatt al-Arab River, which stretches for 200 km along Basrah Governorate. Additionally, the region contains several marshes, situated in the northeastern and northwestern sections. Furthermore, Basrah is situated in the northwestern part of the Arabian Gulf, which constitutes the largest water body in the region (Kadhim et al. 2021).

Climatically, the study area is located within a desert climate region, characterized by two main seasons: a long and extremely hot dry summer, and a moderate temperature and low rainfall winter. Spring and fall are short and transitional seasons between the characteristics of summer and winter (Al-Asadi et al. 2023).

The study area witnessed three wars during the period 1980–2003: the Iran-Iraq War (1980–1988), the First Gulf War in 1991, and the Second Gulf War in 2003. These wars had a significant impact on land use/ land cover in the study area, including the displacement of agricultural lands and wetland drainage projects. In addition, the absence of law enforcement after 2003 led to an increase in population numbers. As well as a noticeable increase in oil production through the substantial expansion of oil field numbers (Ahmed et al. 2022).
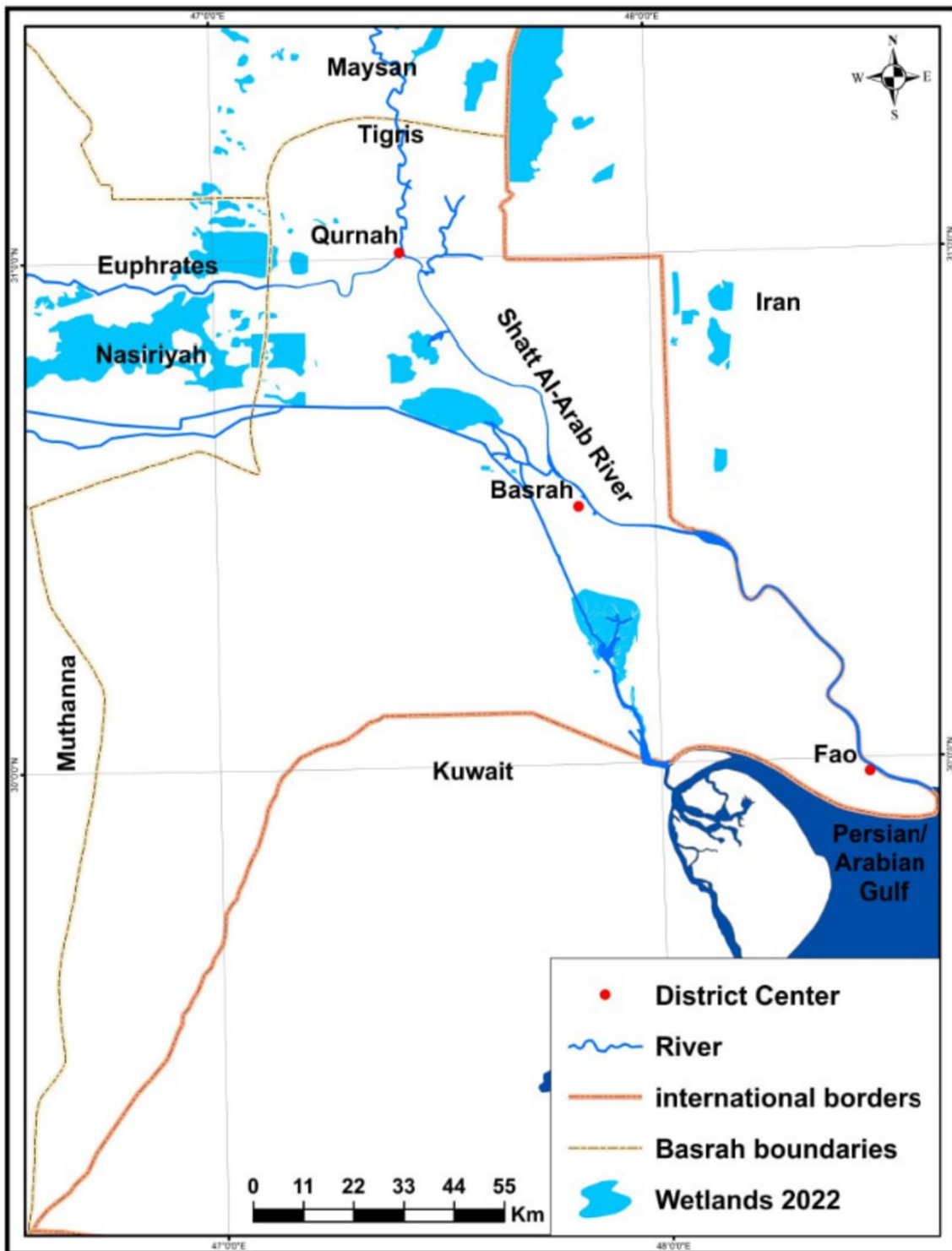
Fig. 1 Map of the study area

The data used

The data utilized in this study comprises historical monthly average temperature data for the period 1948–2022, recorded at the Al-Hussain station in the center of Basrah city (see Fig. 1). To check and validate the temperature data utilized in this study, the temperature data from the Global Land Data Assimilation System (GLDAS) is used. GLDAS

represents a collaborative effort between NASA and international partners, aiming to provide consistent, global datasets of essential land surface variables. These variables encompass soil moisture, temperature, vegetation cover, surface energy, and water fluxes (Rodell et al. 2009). These datasets are created by combining satellite observations, in-situ measurements, and land surface models. The primary goal of GLDAS is to improve our understanding of the water of Earth, energy, and carbon cycles. The land surface model, which orchestrates the exchange of energy, water, and carbon between the land surface and the atmosphere, is at the heart of the GLDAS initiative. This model relies on meteorological inputs like temperature, humidity, and precipitation to generate estimates for critical land surface factors, including soil moisture, evapotranspiration, and surface energy fluxes. As a result of the integration of satellite observations and in situ measurements, the model gains greater precision and spatial resolution. GLDAS datasets are widely used in a variety of applications, including climate and weather modeling, agricultural and water resource management, and natural disaster prediction (Xia et al. 2014). There are four main types of GLDAS models that are used to generate these datasets: Mosaic, Noah, the community land model (CLM), and the variable infiltration capacity (VIC). For the purpose of this study, the Noah model is used. The data of this model

is available from 1948 to the present time (Niu et al. 2011). Model physics is improved and land surface variables are added to this updated version of the Mosaic model (Niu et al. 2011). The basic statistical analysis of monthly temperature data of Noah model is also presented in Table 1. The correlation coefficient between the temperature measurements taken in situ et al.-Hussain station and the Noah model registers a robust value of 0.99 (refer to Fig. 2). This outcome signifies that despite the Noah data being a simulated model, its monthly temperature predictions are remarkably precise and reliable for practical utilization.

The areas of wetlands and green cover were identified by analyzing the satellite images of Landsat 7 and 8 using the normalized difference vegetation index (NDVI) and the normalized difference water index (NDWI). The areas of residential areas and oil fields were identified by using supervised and unsupervised classification and visual interpretation of the same satellite images for the period 1980–2022.

Modeling approaches

To investigate the relationship between temperature and the potential influencing factors, the following modeling approaches were used: univariate time series analysis, trend analysis, and feature selection. Time series decomposition

Table 1 Statistical analysis of monthly average of temperature

Variable	Mean	StDev	CoefVar	Minimum	Median	Maximum	Skewness	Kurtosis
Temperature (based-station measurement) °C	25.322	8.797	34.74	7.200	26.300	41.500	− 0.09	− 1.35
Temperature (Noah model) °C	25.621	9.001	35.13	7.438	26.569	42.888	− 0.11	− 1.35

StDev standard deviation, *CoefVar* coefficient of variation

Fig. 2 Correlation between the monthly temperature from in situ measurement and Noah model

$y = 0.978x + 0.3923$
$R^2 = 0.9855$

Monthly tempeature average (Noah model)

Monthly temperature avearge (in situ-measurment)
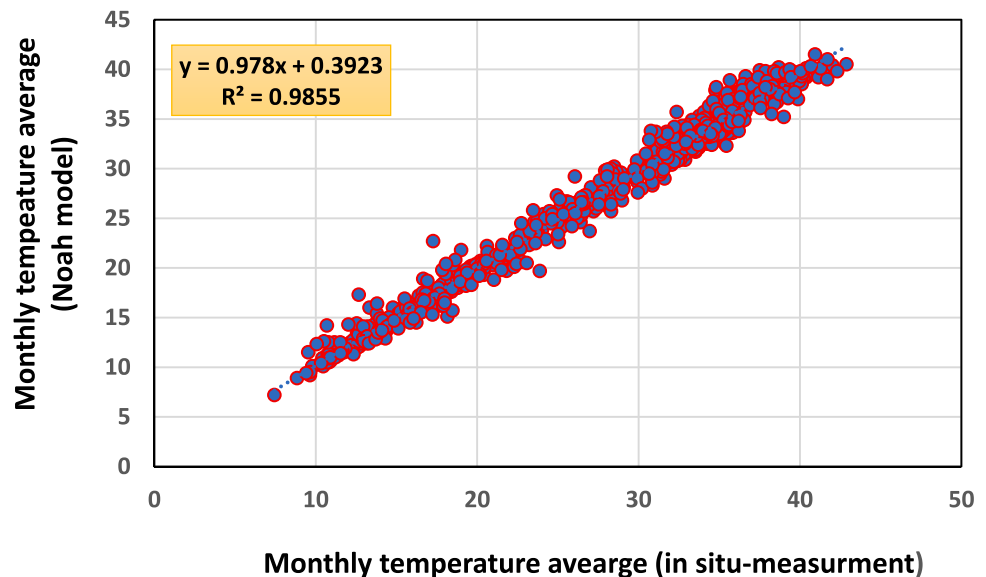
is crucial in understanding and analyzing temporal data, as it disentangles the underlying components such as trend, seasonality, and residual variations, aiding in a more insightful interpretation of the observed patterns (Talagala and Athanasopoulos 2018). Time series trend analysis focuses on identifying and understanding the long-term directional movement in the data, providing valuable insights into underlying patterns or anomalies (Chatfield and Xing 2019). Feature selection, on the other hand, is vital for enhancing model efficiency and interpretability by identifying the most relevant variables that contribute significantly to the predictive performance (Guyon and Elisseeff 2003). Efficient feature selection helps in reducing dimensionality and improving model accuracy, making it an essential step in time series analysis. Integrating these methodologies allows for a comprehensive understanding of temporal data, aiding in informed decision-making and prediction accuracy.

More information about the modeling approach used here is provided below.

Time series decomposition

Time series decomposition is a statistical method that breaks down a time series into its trend, seasonality, and residual components (Talagala and Athanasopoulos 2018). This can be helpful for understanding the underlying patterns and trends of the data, and for forecasts. The trend component represents the overall direction of the series, which can be positive, negative, or no trend. The seasonal component refers to regular, consistent fluctuations in the series, such as those that occur at specific times of the year (Verbesselt et al. 2010). The residual component of a time series represents the random fluctuations that are not accounted for by the trend, cycle, or seasonal components. There are several main types of time series decomposition methods such as classical decomposition, seasonal-trend decomposition using loess (STL), Error-trend-seasonality (ETS), wavelet decomposition, Fourier decomposition, Hodrick-Prescott filter, and moving average (Talagala and Athanasopoulos 2018). The most popular technique among them is STL method. The STL is a statistical method for decomposing a time series into its trend, seasonal, and residual (noise) components. This method was developed by Cleveland and Devlin (1988) as an alternative to the classic decomposition methods such as the X-11-ARIMA algorithm (Ladiray and Quenneville 2012) and the moving average method. The method works as follows (Cleveland et al. 1990): (1) the time series data is made smoother using a special type of local regression called LOESS. This step cleans the data, getting rid of short-term noise and ups and downs. It leaves us with the main trend and the repeating seasonal pattern. (2) The main trend is figured out by doing more LOESS smoothing on the cleaned data. By comparing this smoothed trend with the original data, the repeating seasonal pattern can be figured out.

(3) Finally, the noise is found by taking away the main trend and the seasonal pattern from the original data.

Trend analysis

To study the trend of time series of monthly average temperature, the non-parametric Mann–Kendal (M–K) test and Sen's slope estimator are adopted. The M–K test is a statistical method which is used to detect trends in time series data. It assesses whether there is a significant upward or downward trend in a dataset over a given time period (Sang et al. 2014). The test is particularly useful in environmental and climate studies to identify trends in variables such as temperature, rainfall, and other time-dependent measurements. The M–K test involves comparing the values of a variable at different time points to determine if there is a consistent pattern of increase or decrease (Pohlert 2016). The test takes into account the order of observations and computes a statistic based on the number of concordant and discordant pairs of data points. The null hypothesis of the Mann–Kendall test states that there is no trend in the data, while the alternative hypothesis suggests the presence of a trend. The significance level (α) determines whether the observed trend is statistically significant, or not.

Mathematically speaking, The Mann–Kendal test statistics (S) is calculated as:

$$S = \sum_{k=1}^{n-1} \sum_{j=k+1}^{n} sgn(x_j - x_k) \tag{1}$$

where n denotes the number of observations, and x_k and x_j denote the data values at times k and j. The sign function is defined as follows (Karpouzos et al. 2010):

$$sgn(x_j - x_k) = \begin{cases} +1 & if\ (x_j - x_k) > 0 \\ 0 & if\ (x_j - x_k) = 0 \\ -1 & if\ (x_j - x_k) < 0 \end{cases} \tag{2}$$

The variance can be calculated as follows:

$$var(S) = \frac{n(n-1)(2n+5) - \sum_{i=1}^{m} t_i(t_i - 1)(2t_i + 5)}{18} \tag{3}$$

where m denotes the number of tied groups (a collection of sample data with the same value) and t_i denotes the number of ties of extent i (Gocic and Trajkovic 2013). When the sample size is greater than 8, the standard normal test statistics Z_s is calculated as follows:

$$Z_s = \begin{cases} \frac{S-1}{\sqrt{var(S)}}, & if\ S > 0 \\ 0 & if\ S = 0 \\ \frac{S+1}{\sqrt{var(S)}}, & if\ S < 0 \end{cases} \tag{4}$$

Positive and negative Z_s values represent upward and downward trends, respectively.

The Sen's slope estimator, on the other hand, is a non-parametric statistical technique used to estimate the magnitude of a linear trend in a dataset (Sen 1968). It is particularly useful for analyzing time series data or data sets where the assumption of normality is not met. Sen's slope provides a robust estimate of trend direction and magnitude, even in the presence of outliers or skewed data (Theil 1950). In Sen's slope estimation, the median of all possible slopes between data points is computed (Al-Mohammdawi et al. 2022). This process ensures that extreme values or outliers do not excessively influence the estimation, making it a resistant and robust method for trend analysis.

Sen's slope estimator is primarily used to calculate change per unit time(Sen 1968):

$$Q_i = \frac{x_j - x_k}{j - k} \quad for\ i = 1, \dots, N. \tag{5}$$

The N values of Q_i are ranked from smallest to largest and the Sen's slope is computed as:

$$Q_{med} = \left\{ \begin{array}{ll} Q\big[(N+1)/2\big] & if\ N\ is\ odd \\ \frac{Q[N/2]+Q[(N+1)/2]}{2} & if\ N\ is\ even \end{array} \right\} \tag{6}$$

The sign of Q_{med} refers to the trend's orientation, while its value reflects the steepness of trend.

Feature selection

Feature selection is a process of choosing a subset of features from a dataset that are most relevant to the target variable. The goal is to improve the performance and interpretability of machine learning models by removing irrelevant or redundant features. There are three main types of feature selection methods (Al-Bawi et al. 2021): (1) *Filter methods* use statistical measures to rank features based on their importance. These methods are relatively fast and easy to implement, but they can be insensitive to the specific machine learning model which is used. (2) *Wrapper methods* search for the optimal subset of features by iteratively adding or removing features based on their performance on a holdout dataset. These methods can be more accurate than filter methods, but they can be computationally expensive. (3) *Embedded methods* combine feature selection and model training into a single process. These methods can be very efficient, but they can be difficult to interpret.

The choice of feature selection method depends on the specific problem and the available resources. In general, filter methods are a good choice for speed and simplicity, wrapper methods are a good choice for accuracy, and embedded methods are a good choice for efficiency. For the purpose of this study, the usefulness of the factors for determining the temperature was examined in this study using the Pearson's correlation coefficient (r). r is a measure of the linear correlation between two variables x and y. r is the covariance of the two variables divided by their standard deviations.

$$r_{x,y} = \frac{cov(x.y)}{\sigma_x \sigma_y} \tag{7}$$

where cov is the covariance, σ_x is the standard deviation of x, σ_y is the standard deviation of y. The change of temperature in Basrah can be attributed to different main reasons that include: global warming, vegetation cover and wetland areas reduction, urban area and oilfield expansion. Table 1 shows how these factors changing with time for three years 1980, 2000, and 2022.

For applying feature selection method, WEKA 3.8 software was used. WEKA is an open-source ML software that can be accessed through a graphical user interface, standard terminal applications, or a Java API. It includes a variety of cutting-edge algorithms for common machine and statistical learning problems and is frequently utilized in education, research, and industrial applications.

Results and discussion

Basic statistical analysis of temperature data

A basic statistical analysis of the temperature data is summarized in Table 1. The histogram of the data is presented in Fig. 2, along with a normal distribution. The minimum, maximum, and mean temperatures of the based-station data are 7.2 °C, 41.5 °C, and 25.3 °C, respectively. The median temperature is 26.3 °C, different from the mean, indicating that the probability distribution of the monthly temperatures is not perfectly normal. The standard deviation is 8.8, which implies that approximately 68% of the temperatures in the dataset fall within 1 standard deviation of the mean, or between 16.5 °C and 34.1 °C. The coefficient of variation is 34.74%, which signifies that the standard deviation is relatively large compared to the mean, suggesting that the data is spread out over a wide range of values. The skewness is negative (− 0.09), which indicates that the temperature distribution is slightly left-skewed. It means that there are more values below the mean than above it. Lastly, the kurtosis is also negative, − 1.35, which suggests that the probability distribution of temperature is platykurtic, meaning it is flatter than a normal distribution. Accordingly, it can be inferred that the probability distribution of temperature is not normal; instead, it exhibits a slight left-skew. The Noah temperature data exhibits approximately the same values of the statistical

parameters as the station-based, therefore, there is no need to discuss the obtained values (Fig. 3).

Time series decomposition findings

The additive components of the temperature time series are shown in Fig. 4. The R programming language was used to analyses the data and produce the figure. The temperatures appear to have an upward trend suggesting that the average temperatures have generally increased over the years. There are some periods of slight decrease or fluctuations in the trend, but the overall pattern points to a warming trend. The variability in the trend could be due to various factors, including climate cycles, global warming, and local weather conditions. The seasonal component values seem to vary for each month across different years. For instance, there's a recurring pattern of higher values in May, June, and July (around 6.13–11.01 °C), which could correspond to the warmest months of the year. On the other hand, the values for the remaining months are mostly negative, suggesting lower values during the colder months. Looking at the values of the residuals. It appears that they vary from small to relatively moderate values. In some years, the residuals are closer to zero, indicating that the observed values align well with the trend and seasonal components. In other years, the residuals deviate more, suggesting that there are unexplained factors affecting those particular years. While there isn't a clear pattern in the residuals across the months or years, there are some periods where the residuals seem to consistently deviate from zero. For example, there are stretches of years where the residuals are consistently positive or negative. This might indicate the presence of other factors that influence the data and are not captured by the trend and seasonality. The residuals show fluctuations throughout the years, which might represent short-term variations or unexpected events that couldn't be accounted for by the trend

and seasonal patterns. Finally, the residuals don't appear to accumulate over time, which suggests that the trend and seasonality components capture most of the systematic patterns in the data.

Trend analysis

The result of applying Mann-Kendal test and Sen's slope estimator is shown in Table 2, from which it can be seen that the z-statistic, which represents the test statistics for the Mann-Kendal test, is 5.3891, is greater than the critical value of 1.96 for a two-tailed test at the 0.05 significance level. Therefore, we can conclude that there is a statistically significant trend in the data set. The p-value is $7.083e^{-08}$, which is less than 0.05. This means that there is less than a 0.05% chance of obtaining a z-statistic that is at least as extreme as the one observed in the data set if the null hypothesis is true. Therefore, we can reject the null hypothesis and conclude that there is a statistically significant trend in the data set. The S represents the Mann-Kendal trend statistic. A positive value indicates an increasing trend, a negative S value indicates a decreasing trend, and S value of 0 indicates no trend. In our case, the S value is 5. $5.549000e^{+04}$, which is positive. Therefore, we can conclude that there is an increasing trend in the data set. The varS represents the variance of the Mann-Kendal trend statistics and mainly used to calculate the confidence interval for the trend statistic. The tau represents the Kendall's tau, which is a non-parameter measure of correlation. A positive tau value indicates an increasing trend, a negative tau value indicates a decreasing trend, and a tau value of 0 indicates no trend. In this case, the tau value is $1.149506e^{-01}$, which is positive. Therefore, we can conclude that there is an increasing trend in the data set. Finally, the Sen's slope value is 0.00475, which is positive. Therefore, we can conclude that there is an increasing trend in the data set. There is a possibility of uncertainty in
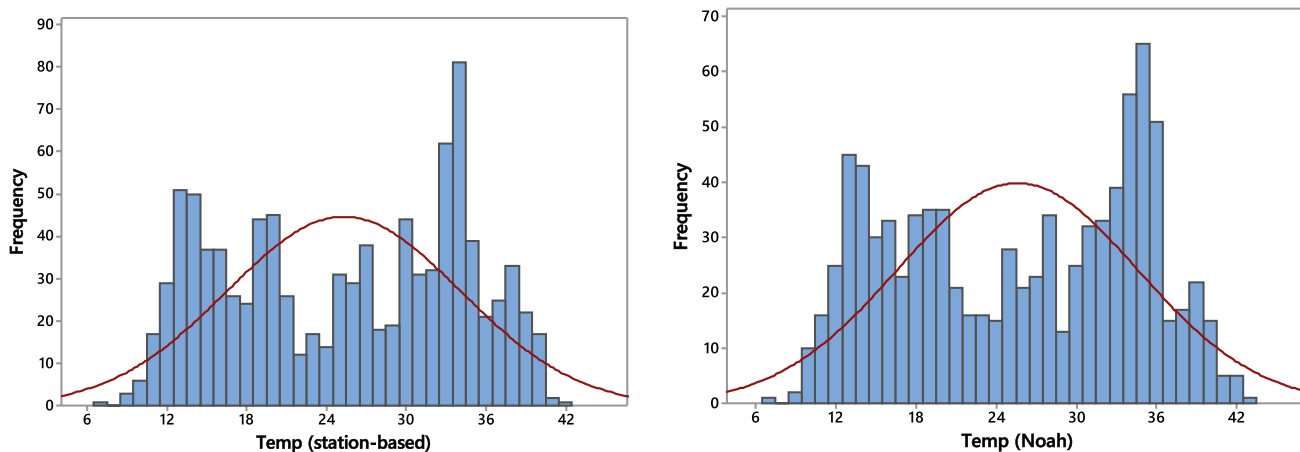
Fig. 3 Histogram and normal curve for the monthly temperature (station-based and Noah model)
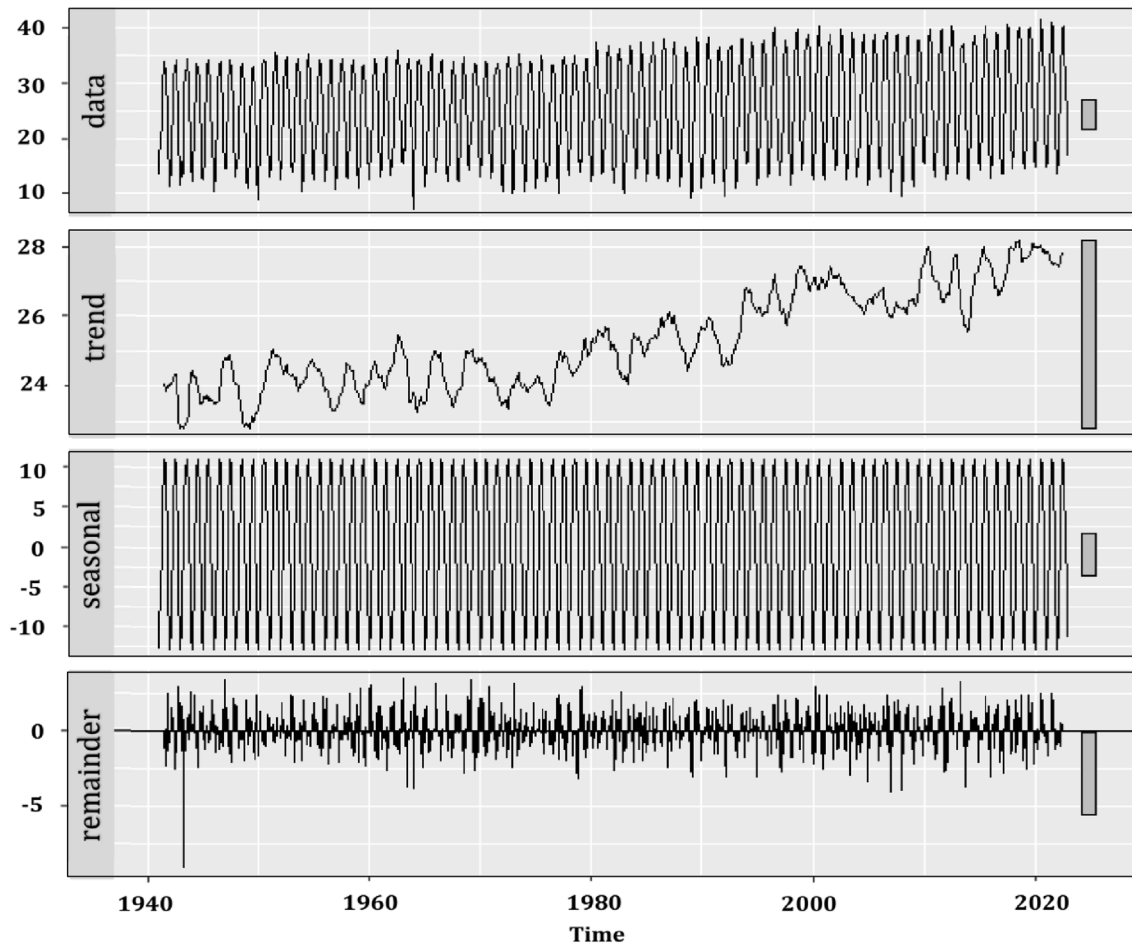
Fig. 4 Additive components of the monthly temperature time series

Table 2 Results of trend analysis

Test	Z	n	p-value	Alternative hypothesis	Sample estimates		
					S	VarS	Tau
Mann-Kendal	5.3891	984	7.08e^{-08}	true S is not equal to 0	5.5489e^{04}	1.0602e^{08}	1.1494e^{-01}
Sen's slope	5.3891	984	7.09e^{-08}	true z is not equal to 0	Sen's slope$=0.0047$		

the obtained results, which may arise from various factors, the most important being: (1) Sample size: The sample size is large (984 in this case, generally considered significant), which reduces uncertainty in the accuracy of the results. (2) Both tests assume that the data should be independent, with no autocorrelation. Violating these assumptions may lead to inaccurate results. The Autocorrelation plot, Fig. 5 shows that most of the calculated autocorrelation values are close to 1 or -1, indicating the presence of autocorrelation between the monthly temperature values. This could introduce uncertainty into the computed trend value. (3) While statistical tests provide evidence of the existence of a trend, they do not explain the reasons behind this trend. External

factors are not considered here, and they may contribute to the observed variations.

Overall, both tests indicate that there is a statistically significant increasing trend in the dataset. The trend is estimated to be 0.00475 per month; thus, for the whole period of the study (74 years) the temperature is increasing about 4.218 °C. Since the average temperature in Basrah has reached 25.3 °C, the climate change has contributed to a temperature increase by a percentage of 16.67%. Apparently, temperature increase in Basrah is alarmingly high, especially when compared to the global average temperature increase of 1 °C over the past century. This suggests that Basrah is experiencing a much more rapid rate of warming than the

Fig. 5 Autocorrelation function to detect trend analysis uncertainty
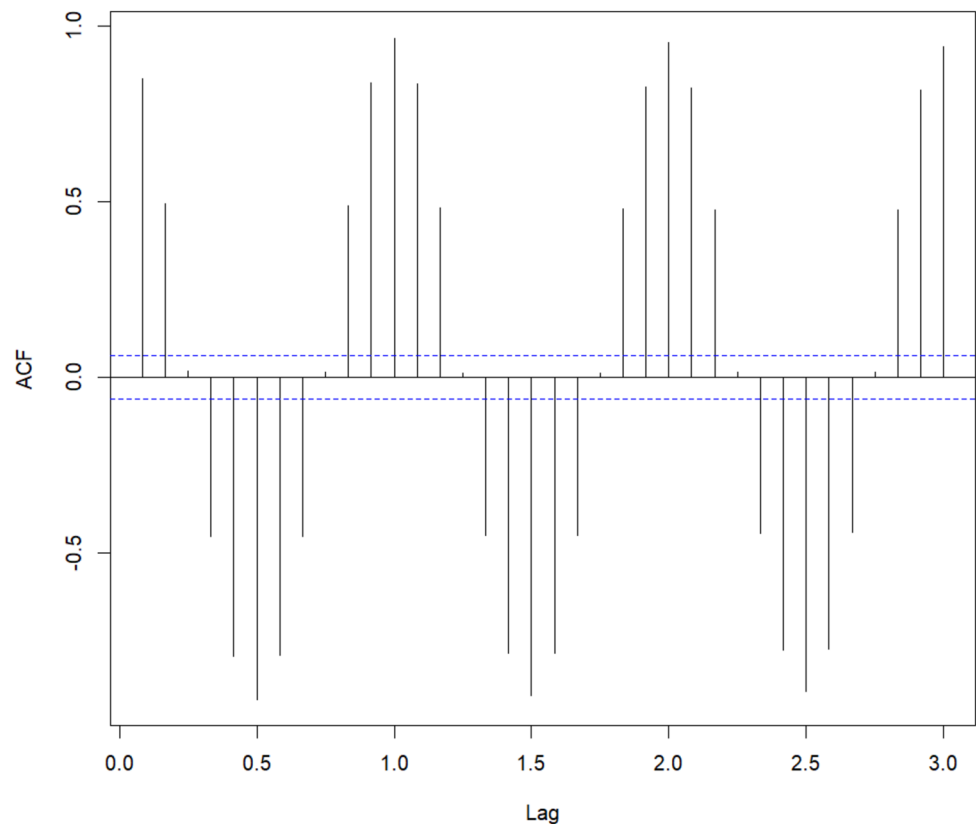
rest of the world. It is important to investigate the causes of this temperature increase in order to mitigate its effects and prevent further damage to the region.

Possible causes of the temperature rising

Global warming

The climate of the study area is inevitably affected by the global climate system, as it is part of the Earth's surface. However, the effects of climate change vary across the Earth's surface (Zhang et al. 2000, 2014; Partal and Kahya 2006). For example, the global average temperature has increased by 0.18–0.74 °C between 1906 and 2005 (IPCC 2014), but the average surface air temperature of the Earth has increased by about 1 °C since 1880 (Stocker 2014). More than half of this increase has occurred since the mid-1970s. Indirect temperature estimates suggest that the period from 1989 to 2019 was very likely the warmest in over 800 years, and the most recent decade, 2010–2019, was the warmest decade since 1850 (National Academy of Sciences 2020). The average temperature of the air on Earth's surface is estimated to be around 15 °C (Poulopoulos and Inglezakis 2016) and global warming has contributed to a 6.66% increase in this temperature. This increase is due to a number of factors, including human activities that release greenhouse gases into the atmosphere. Greenhouse gases trap heat from the sun, which causes the Earth's atmosphere to warm.

The Middle East region, including the study area, is one of the regions that are most affected by the global climate change. It is expected to experience a temperature increase of up to 2 °C in the next 15–20 years (Osman-Elasha 2010; Mansouri Daneshvar et al. 2019). The study area has been particularly affected by temperature changes due to its tropical location and its proximity to oil-producing countries. In the past 74 years, the temperature in the study area has increased by 4.218 °C, which is 4.2 times the global average temperature increases of 1 °C. This suggests that there are local factors that contribute to the sharp increase in temperature rates in the study area. Therefore, the temperatures rising fact of Basrah is even more perilous than in the rest of the Middle East. Table 3 shows how the global average temperature has evolved over time along with other factors believed to impact a region's temperature regime.

Green spaces reduction

Green cover plays an important role in regulating temperatures, especially the minimum and maximum temperatures. When plants absorb water from the soil, they release most of it into the atmosphere as water vapor through a process called transpiration (Morison et al. 2008). Although water

Table 3 Factors affecting temperature rise

Change percentage (1980–2022)	Year					Factor
	2022	2010	2000	1990	1980	
5.33	16.00	15.62	15.30	15.35	15.19	Global warm (°C)
-83.61	422.12	888.50	1081.01	1115.33	2575.59	Greens pace areas (km²)
-81.94	2006.54	3766.00	646.13	5776.00	11,114.66	Wetland area (km²)
85.33	1297.50	1235.70	933.10	896.60	700.10	Oil fields area (km²)
222.38	243.69	141.15	124.14	111.26	75.59	Residential area (km²)
10.16	27.85	27.90	26.78	25.90	25.28	Average temperature (°C)

vapor is a greenhouse gas, representing approximately 60% of the total greenhouse effect (Poulopoulos and Inglezakis 2016), it helps to moderate temperatures by absorbing and emitting radiation from the sun (Allan 2012). This reduces the amount of heat that reaches the Earth's surface. In addition, dense plant canopies provide shade, which prevents sunlight from reaching the ground (Rago et al. 2021). This also helps to keep temperatures cooler.

In order to meet their water needs, agricultural plants frequently require irrigation; nevertheless, irrigation water has little impact on global average temperatures (Sacks et al. 2009). Nevertheless, agricultural irrigation significantly affects maximum temperatures. This effect is especially apparent on the hottest days of the year (Thiery et al. 2017; Chou et al. 2018). In irrigated areas, irrigation water reduces surface temperatures by increasing evaporation caused by moist soil (Boucher et al. 2004; Haddeland et al. 2006; Li et al. 2017). A balance between transpiration and carbon dioxide consumption occurs in plants (Alam et al. 2019). Therefore, the deterioration of the plant cover and the reduction of transpiration processes contribute to an increase in the concentration of one of the most important greenhouse gases in the atmosphere.

The vegetation cover in the study area has experienced a sharp decline over the past four decades. Basrah province was once teeming with date palms, to the extent that it was considered one of the largest date palm forests in the world (Al-Asadi and Muttashar 2022). However, it has now become almost barren, with the green cover area shrinking from 2,575.59 km² in 1980 to 422.12 km² in 2022, indicating a 83.61% decline in green cover area (Fig. 6 and Table 3). The reasons for this decline can be attributed to the high salinity of water and soil in the region, urban sprawl on agricultural land, and the absence of effective agricultural policies, especially during the period 2003–2022.

Wetland area reduction

Marshes are one of the most important types of wetlands, characterized by shallow waters and abundant vegetation. Iraq's marshes represent the largest ecosystem in the Middle East and West Asia, making them among the world's most significant wetlands (Partow 2001). Iraq's marshlands are located in the southern regions, extending in a triangular shape between three provinces: Maysan, Thi Qar, and Basrah. The areas of marshland (including wetlands) range from 15,000 to 20,000 km² (Partow 2001; Alwash et al. 2004; Albarakat et al. 2018).

The marshlands fulfill significant ecological roles, notably by influencing the local climate through their effective ability to capture carbon dioxide (a major greenhouse gas) from the atmosphere and sequestering it within the soil. This action aids in alleviating climate warming (Gedan et al. 2011). These marshlands also create exceptionally humid environments through the process of evapotranspiration, augmenting moisture levels in the neighboring air. This phenomenon serves to cool the air, moderate the climate, and alleviate the impact of arid conditions on the local weather (Wong et al. 2017). Reports from the Iraqi marshland areas indicate a notable reduction of up to 5 °C in summer temperatures. Moreover, the marshlands play a role in curtailing the occurrence of dust storms (Iraqi Ministries of Environment 2006).

The wetlands in southern Iraq were intentionally desiccated between 1980 and 2000, leading to a 90% reduction in their area (Alwash et al. 2004). According to the aerial photographs used in the current study to detect the temporal variation in wetland area for the years 1980, 1990 2000, 2010 and 2022, the wetland area varied from approximately 11,115 km² in 1980 to about 2,007 km² in 2022, resulting in an 81.94% reduction in wetland area (Table 3 and Fig. 7). After 2003, the Iraqi government sought to revive the wetlands, but the sharp decrease in the discharge of the Tigris and Euphrates rivers from 78 km³ in 1977 to 18 km³ in 2022 posed a barrier to feeding vast areas of the wetlands. The significant reduction in wetland area must have important implications for the local climate by reducing actual evapotranspiration rates and increasing temperatures, especially during the summer (Partow 2001). It is worth noting in this regard that rainwater falling on the city of Basrah used to accumulate in low-lying vacant lands to form ponds, and its duration would continue until the end of the summer, believed to contribute to cooling the air and reducing temperature. However, these ponds have clearly shrunk in both
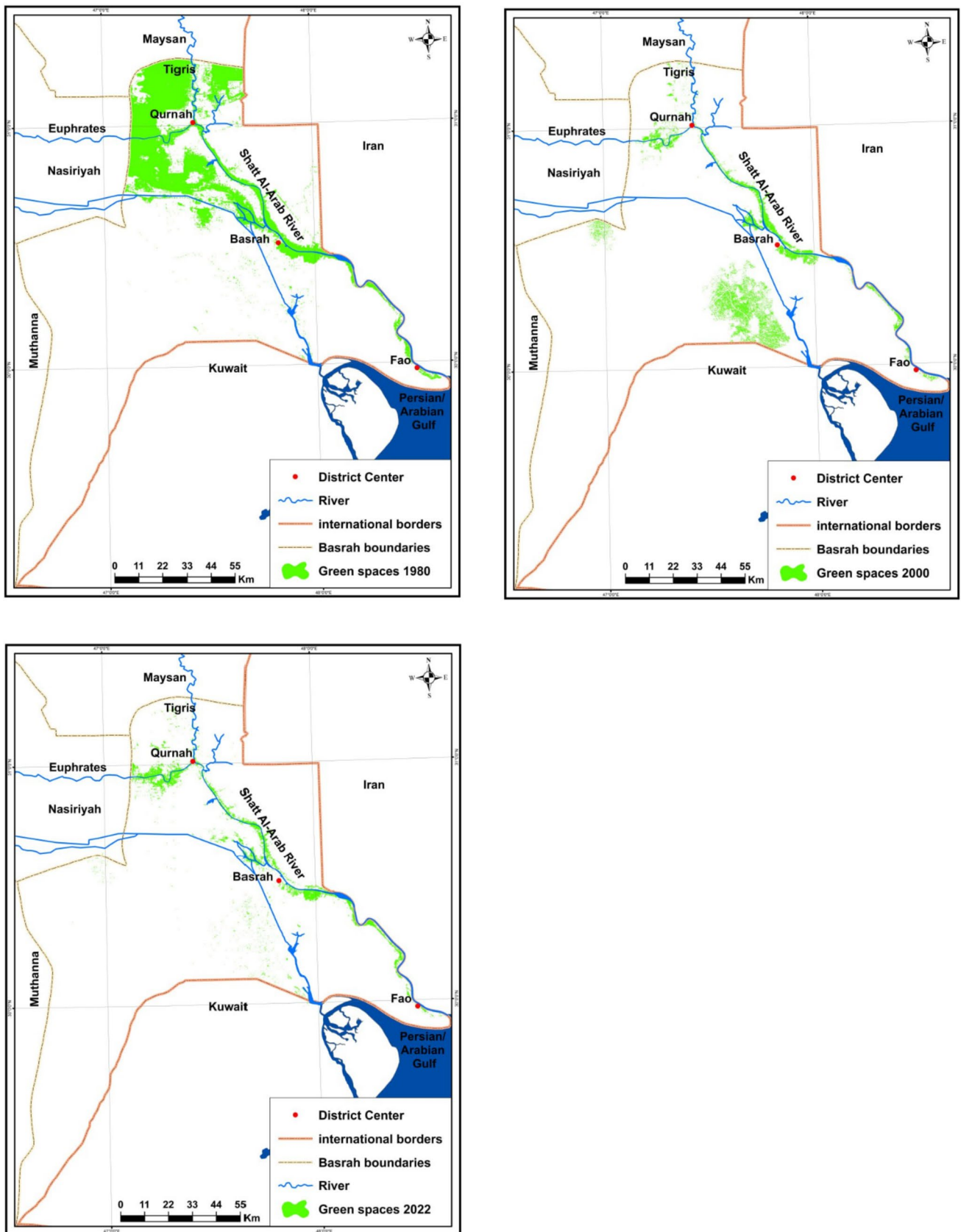
Fig. 6 The area of green cover change over time (42 years) at three dated stages June 1980, June 2000, and June 2022 in Basrah province
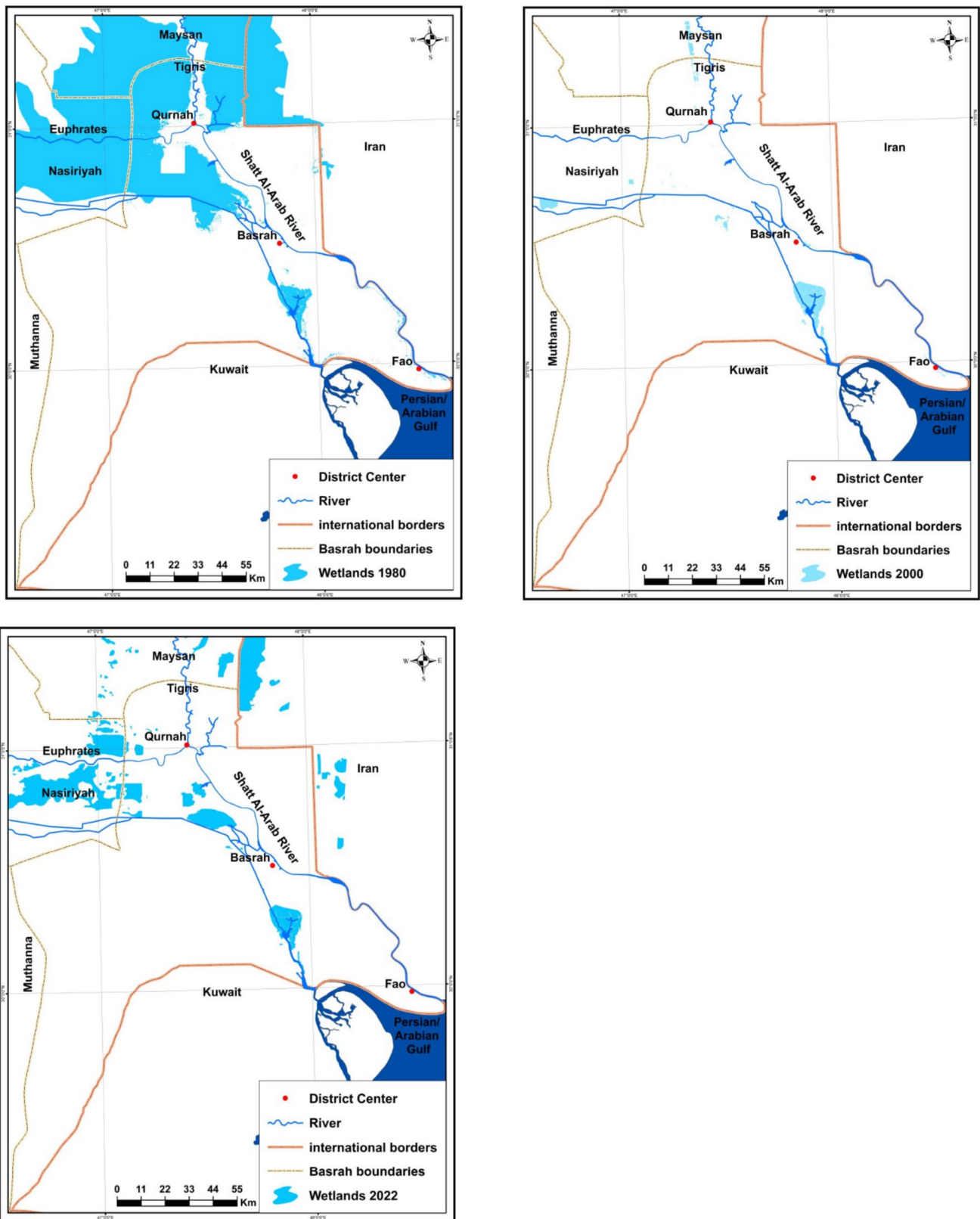
Fig. 7 The wetland areas change over time (42 years) at three dated stages June 1980, June 2000, and June 2022 in southern Iraq

area and duration in recent years, and this may be attributed to the expansion of urban areas, particularly unregulated construction, as well as a decrease in groundwater levels, in addition to an increase in evaporation rates.

Oilfield area expansion

The development of civilization has been paralleled to the increased burning of fossil fuels. These fuels are used for industrial processes, energy generation, transportation, and other activities that elevate the concentration of greenhouse gases in the atmosphere (Pachauri et al. 2014). The processes involved in oil extraction and energy production release numerous gases, including carbon dioxide (CO_2), methane (CH_4), and nitrous oxide (N_2O), all of which contribute to the escalation of atmospheric temperatures (Philander 2008). This is because these greenhouse gases have the capacity to absorb infrared radiation (Pachauri et al. 2014). Moreover, the oil industry emits various gases such as carbon monoxide (CO), sulfur oxides (SO_x), nitrogen oxides (NO_x), and methane (CH_4) (Lazaridis, 2011). Crude oil consists of a blend of carbon, hydrogen, sulfur, and some minerals (Change 2006).

Crude oil production is the main factor in the industrial and economic sector in Iraq, as it heavily relies on the use of fossil fuels to generate electricity. There are four types of fuels used in electricity production in Iraq; natural gas, crude oil, diesel, and renewable energy sources, which represent 50%, 28%, 15%, and 7% of those sources, respectively (Jassim et al. 2016). During the combustion process, the carbon and hydrogen elements in fossil fuels are converted into carbon dioxide and water vapor. Carbon dioxide gas accounts for about 95% of energy emissions, including electricity production (Aalde et al. 2006).

The province of Basrah has witnessed a significant growth in oil production through increasing the number of oil wells and intensifying oil extraction operations. Oil production in the study area has risen from 0.7 million barrels per day during the period of 1995–1998 to about 2.9 million barrels per day during 2015–2021. Temporal analysis of satellite images used in the current study indicates an expansion of the oil industries' footprint (companies and boundaries of oil facilities) from 700.10 km² in 1980 to 1297.50 km² in 2022 (Fig. 8 and Table 3), representing an increase of around 85.33%. However, the increase in oil extraction operations and energy production contributes to an increase in greenhouse gas concentrations in the air of Basrah province, especially since most oil extraction operations involve the flaring of associated natural gas. Iraq ranks second globally, after Russia, in the flaring of associated gas from oil production (World Bank 2022; IEA 2022) as the majority of natural gas reserves in Iraq are associated with oil fields (IEA 2012). The International Energy Agency estimated that in 2019,

Iraq accounted for 9% of all global methane emissions from the oil and gas sector (UNEP 2021).

Residential area expansion

Population growth can directly or indirectly affect climate characteristics. The direct impact is mainly due to the increase in greenhouse gas emissions such as carbon dioxide (CO_2) and methane (CH_4) resulting from transportation and breathing. The indirect impact is primarily due to changes in land use and urbanization (Pachauri and Reisinger 2008), which lead to the expansion of roads and urban areas (Peres et al. 2016). The increase in population leads to an increase in carbon emission that contributes to climate change. Estimates show that CO_2 emissions increase by an annual rate of 1.5%, and cars are among the main activities responsible for carbon emissions (Oke 1982). The expansion of urban areas also increases the impact of urban heat islands, which means an increase in temperature in cities compared to rural areas. In general, the expansion of residential areas in the study area is an important factor in the increase in air temperature through the following axes: (1) *Population growth*: The population in Basrah has increased from about 0.5 people according to the 1977 census to about 3.5 million people according to the 2022 estimates, and the population growth rate is estimated at about 600%. Furthermore, the Basrah province witnessed a huge influx of immigrants during the period 2005–2019, with numbers exceeding one million people from the southern provinces, especially from Maysan and Thi Qar. (2) *Increase in the number of cars*: The Basrah province witnessed a significant increase in the number of cars after 2003. The number of cars increased from about 24,000 vehicles in 1977 to more than 350,000 vehicles in 2022, with a growth rate of about 1358.33%. The Basrah Governorate has a large number of cars and trucks, which are a major source of air pollution and greenhouse gas emissions. (3) *Urban sprawl*: There is no doubt that there is a causal relationship between population growth and the number of residential buildings, according to the aerial images adopted in the current study to detect the spatial variation of residential areas for the years 1980, 1990, 2000, 2010 and 2022, the area of residential buildings increased from 75.59 km² in 1980 to 243.69 km² in 2022, with an estimated increase of around 222.38%.

Figure 9 and Table 3 showed how the residential areas in the Basrah province change with time from 1980 to 2022.

Feature selection

WEKA software supports correlation-based feature selection with the *CorrelationAttributeEval* technique that requires the use of a Ranker search method. The findings of applying this technique in our dataset (Table 3) is shown in Table 4. All
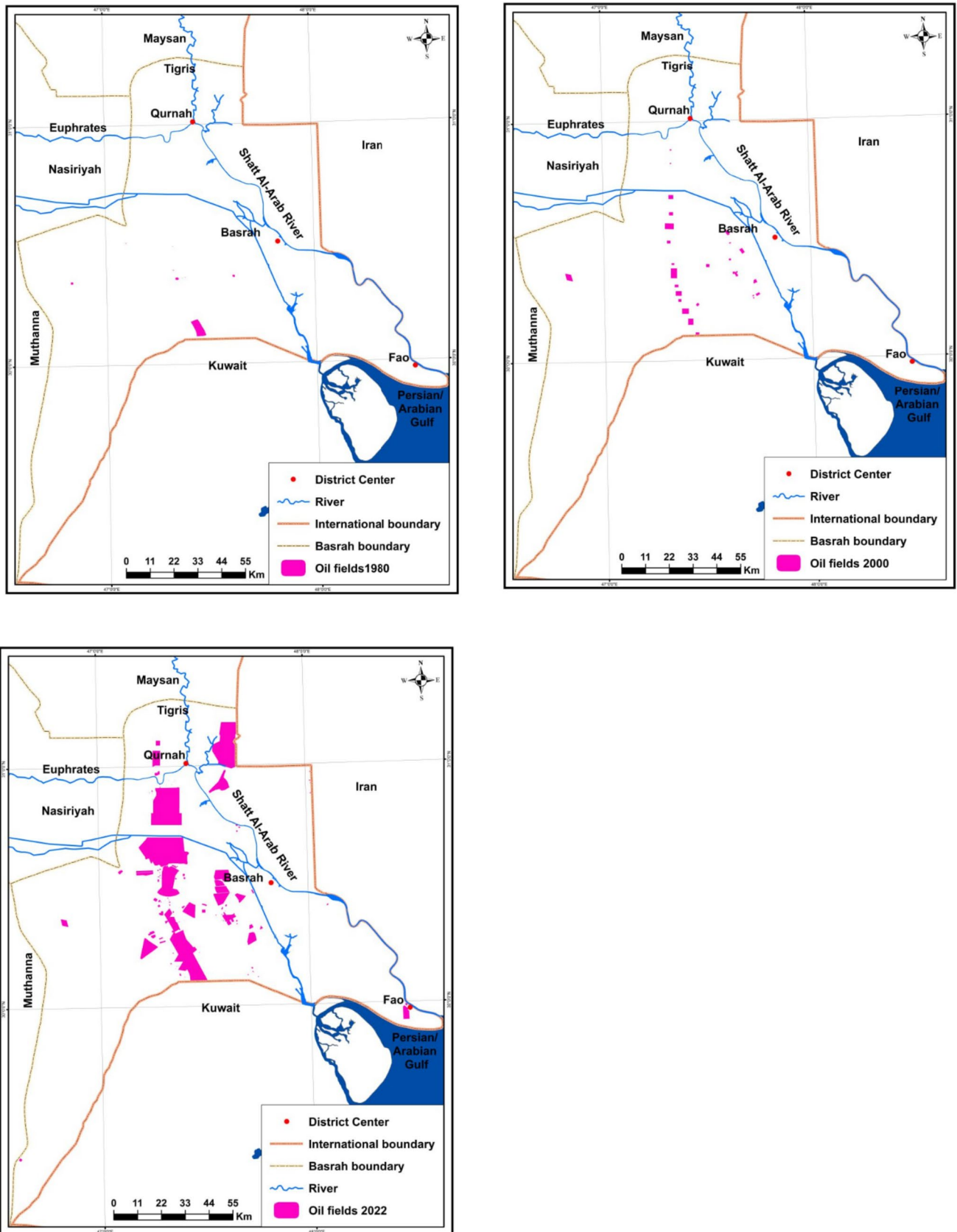
Fig. 8 Areal change of oil fields over time (42 years) at three dated stages 1980, 2000, and 2022 in Basrah province
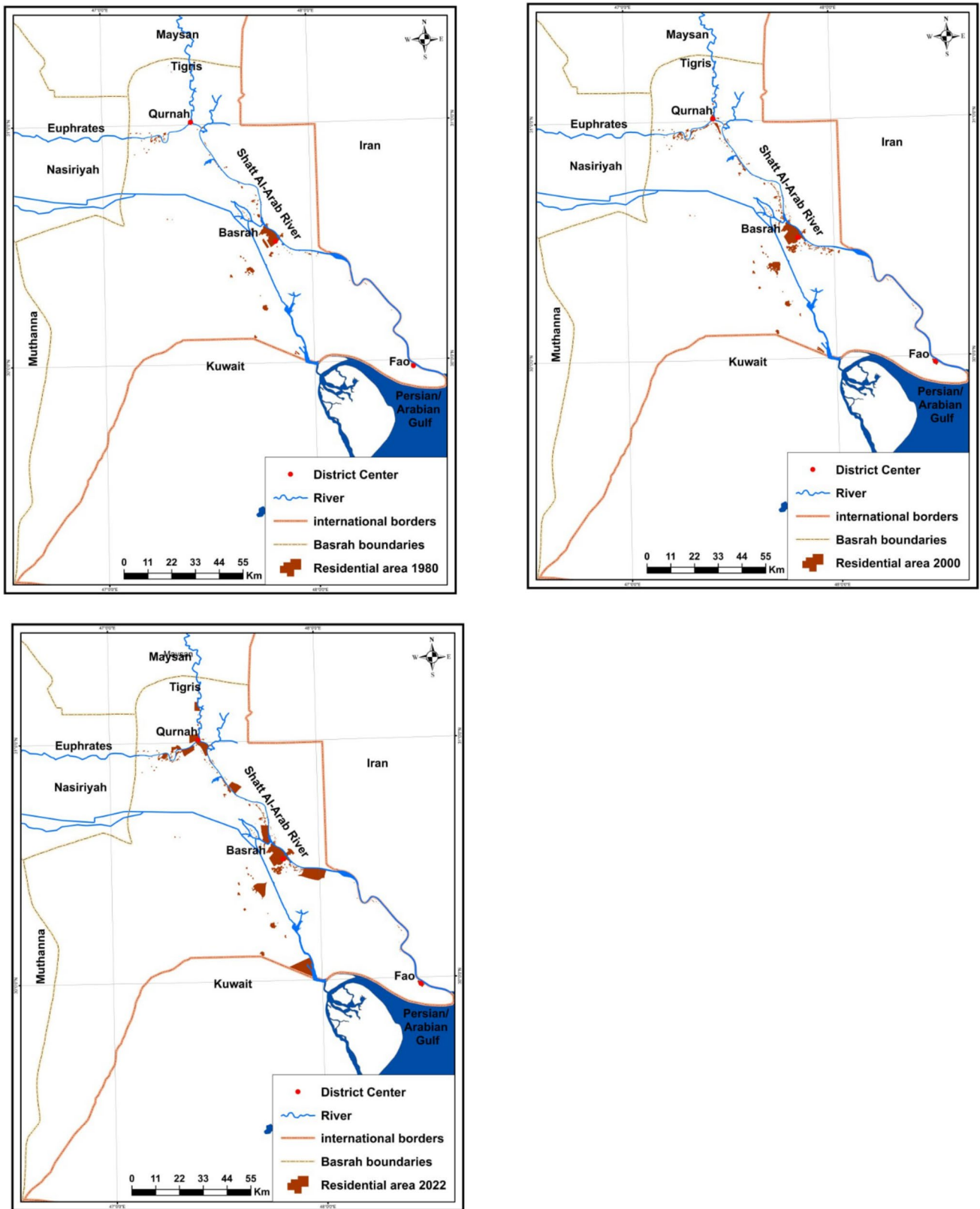
Fig. 9 Residential areas change over time (42 years) at three dated stages June 1980, June 2000, and June 2022 in Basrah province

factors have *r* greater than 0.76, meaning that all have impact of the temperature changes. The most influential factors were oilfield expansion with 0.97 correlation, followed by green space reduction, global warming, urban area expansion, and wetland area reduction with -0.762. The correlation coefficients were positive for oilfield expansion, global warming and urban area expansion, meaning that as these factors increase, the temperature increase as well. Besides, the correlation coefficients were negative for green space reduction and wetland area reduction, meaning that as these factors decrease, the temperature increases, and vice versa. Overall, the expansion of oilfields area and green space reduction seem to be the most factor influencing the temperature changes in the study area.

The results of this study consistent with the findings by Tarawneh and Chowdhury (2018), Mousavi et al. (2020) and Odnoletkova et al. (2020) in considering the increase in greenhouse gas emissions from the energy sector as the primary factor contributing to rising temperatures. However, it differs by identifying the deterioration of vegetation cover in the region as the second major factor rather than urbanization, as suggested by prior studies. Urban expansion, in the current study, constituted the last (fifth) factor in its contribution to temperature increase.

The independent impact of these five factors on temperatures was emphasized in the current study. However, in reality, these factors together contribute to the warming in Basrah Province. Moreover, these factors interact with each other; for instance, urban expansion, oil field growth, and wetland shrinkage have contributed to the decline of green cover. Additionally, global warming has led to the contraction and deterioration of wetlands and vegetation in the study area.

Conclusions and recommendations

Basrah province is characterized by high temperatures, with an annual average temperature of 25.3 °C for the period from 1948 to 2022, due to its tropical location. However, it has experienced a sharp increase in temperature rates, with

Table 4 Feature selection using correlation coefficient (*r*)

Factor	R	dominant factor
Global warming	0.836	3
Green space reduction	− 0.946	2
Wetland area reduction	− 0.762	5
Oilfield expansion	0.970	1
Residential area expansion	0.795	4

monthly average increase of 0.00475 °C per over the past 74 years (4.218 °C in total). This temperature increase is significantly higher than the average temperature increases globally and in the Middle East, which were approximately 1 and 2 °C respectively over the past century. The main causes of the temperature rise in this region are likely linked to local factors, notably the expansion of both oil fields and urban areas, as well as the reduction of green cover and wetlands. Basrah has witnessed a clear change in land use, particularly during the period from 1980 to 2022, attributed to recurrent wars, lack of planning, drought prevalence, and decreasing river water flow. Besides these four local factors, global warming also plays a significant role in driving the temperature increase in the study area.

Despite the multitude and diversity of factors influencing temperature trends in the study area, there was a strong correlation between these five factors and temperature rise, especially regarding the expansion of oil field areas and the reduction of green cover. This strongly suggests that local factors (changes in land use) have a more significant impact on temperature increase in the region compared to global warming. These various factors interact with each other and merge together to influence temperature levels. If this interaction and impact continues at the same intensity, it will lead to an increase in temperatures and warming in the Basrah Provence, potentially causing a genuine environmental disaster. The contribution of changes in land use to temperature trends depends on the type of land use and its spatial expansion or reduction. However, attempting to determine the extent of contribution of local factors to the temperature rise can aid decision-makers in implementing necessary methods and strategies to mitigate climate change, both within Basrah province and in regions and provinces facing similar conditions to the study area.

Among the most important recommendations of the study are: (1) to take steps to mitigate the effects of climate change and adapt to the changes that are already occurring. This will require a coordinated effort from governments, businesses, and individuals. It is necessary to accelerate the expansion of green cover by planting perennial trees, such as palm trees, and encouraging citizens to cultivate agriculture to achieve environmental balance. Special laws should be issued for this purpose. (2) To limit the horizontal expansion of population areas, especially towards agricultural lands in the districts and sub-districts, and focus on vertical construction while restricting slums. (3) To pursue measures to limit the influx of migration to Basra Governorate. (4) To preserve wetlands (marshes), even if the government is forced to fill marsh areas with saltwater, such as drainage water. (5) To work to reduce the drilling of new oil wells and seek investments in technologies that can capture gases associated with oil extraction. (6) To reduce emissions from car exhausts and encourage citizens to use public transport. The government

should also consider reducing the import of fuel-powered cars and promote the use of hybrid cars (HYBRID) to minimize emissions.

Data availability Data will be made available on request.

Declarations

Conflict of interest The authors declare that they have no competing financial interests or personal relationships that may have influenced the work reported in this study.

References

Aalde H, Gonzalez P, Gytarsky M et al (2006) Forest land. In: Eggleston HS, Buendia L, Miwa K, Ngara T, Tanabe K, editors. 2006 IPCC guidelines for national greenhouse gas inventories, prepared by the national greenhouse gas inventories programme. Hayama, Japan: IGES. 4.1–4.83

Ahmed MD, Abdulhasan MM, Taher Braiber H et al (2022) The effect of oil prices, oil demand, oil licensing round, oil product capacity, oil sector development, and inflation on the economic development of Iraq's economy. AgBioForum 24(1):153–160

Alam MS, Lamb DW, Rahman MM (2019) In-situ partitioning of evaporation and transpiration components using a portable evapotranspiration dome—a case study in Tall Fescue (Festuca arundinacea). Agric Water Manag 213:352–357

Al-Asadi SAR, Muttashar WR (2022) Impact of the environmental degradation of rivers on the reappraisal of international agreements related to the transboundary watercourse, Shatt Al-Arab River (Southern Iraq): a case study. Sustain Water Resour Manag 8:84

Al-Asadi SAR, Alhello AA, Ghalib HB et al (2023) Seawater intrusion into Shatt Al-Arab River, Northwest Arabian/Persian Gulf. J Appl Water Eng Res 11:289–302

Albarakat R, Lakshmi V, Tucker CJ (2018) Using satellite remote sensing to study the impact of climate and anthropogenic changes in the Mesopotamian marshlands. Iraq Remote Sens 10:1524

Al-Bawi AJ, Al-Abadi AM, Pradhan B, Alamri AM (2021) Assessing gully erosion susceptibility using topographic derived attributes, multi-criteria decision-making, and machine learning classifiers. Geomatics Nat Hazards Risk 12:3035–3062

Allan RP (2012) The role of water vapour in Earth's energy flows. Surv Geophys 33:557–564

Al-Mohammdawi JA, Al-Abadi AM, Al-Ali AK et al (2022) Assessing the spatial and temporal variations of terrestrial water storage of Iraq using GRACE satellite data and reliability–resiliency–vulnerability indicators. Arab J Geosci 15:1–13

Alwash A, Alwash S, Cattarossi A (2004) Iraq's marshlands-demise and the impending rebirth of an ecosystem. In: Critical transitions in water and environmental resources management, pp 1–9

Boucher O, Myhre G, Myhre A (2004) Direct human influence of irrigation on atmospheric water vapour and climate. Clim Dyn 22:597–603

Buckley LB, Ehrenberger JC, Angilletta MJ (2015) Thermoregulatory behaviour limits local adaptation of thermal niches and confers sensitivity to climate change. Funct Ecol 29:1038–1047

Change IPO (2006) 2006 IPCC guidelines for national greenhouse gas inventories. Inst Glob Environ Strateg Hayama, Kanagawa, Japan

Chatfield C, Xing H (2019) The analysis of time series: an introduction with R. CRC Press

Chou C, Ryu D, Lo M-H et al (2018) Irrigation-induced land–atmosphere feedbacks and their impacts on Indian summer monsoon. J Clim 31:8785–8801

Cleveland WS, Devlin SJ (1988) Locally weighted regression: an approach to regression analysis by local fitting. J Am Stat Assoc 83:596–610

Cleveland RB, Cleveland WS, McRae JE, Terpenning I (1990) STL: A seasonal-trend decomposition. J off Stat 6:3–73

Farooq I, Shah AR, Salik KM, Ismail M (2021) Annual, seasonal and monthly trend analysis of temperature in Kazakhstan during 1970–2017 using non-parametric statistical methods and GIS technologies. Earth Syst Environ 5:575–595

Gedan KB, Kirwan ML, Wolanski E et al (2011) The present and future role of coastal wetland vegetation in protecting shorelines: answering recent challenges to the paradigm. Clim Change 106:7–29

Gocic M, Trajkovic S (2013) Analysis of changes in meteorological variables using Mann-Kendall and Sen's slope estimator statistical tests in Serbia. Glob Planet Change 100:172–182

Guyon I, Elisseeff A (2003) An introduction to variable and feature selection. J Mach Learn Res 3:1157–1182

Haddeland I, Lettenmaier DP, Skaugen T (2006) Effects of irrigation on the water and energy balances of the Colorado and Mekong river basins. J Hydrol 324:210–223

Halder S, Saha SK, Dirmeyer PA et al (2016) Investigating the impact of land-use land-cover change on Indian summer monsoon daily rainfall and temperature during 1951–2005 using a regional climate model. Hydrol Earth Syst Sci 20:1765–1784

Hashim BM, Al Maliki A, Alraheem EA et al (2022) Temperature and precipitation trend analysis of the Iraq Region under SRES scenarios during the twenty-first century. Theor Appl Climatol 148:881–898

Hassan WH, Nile BK, Kadhim ZK et al (2023) Trends, forecasting and adaptation strategies of climate change in the middle and west regions of Iraq. SN Appl Sci 5:312

Hua W, Chen H, Li X (2015) Effects of future land use change on the regional climate in China. Sci China Earth Sci 58:1840–1848

IEA (2012) Iraq Energy Outlook, Paris

IEA (2022) US Energy Information Administration, Iraq Energy Overview, 2022, Country Analysis Executive Summary, Iraq

IPCC (2014) Climate change 2014: synthesis report (SYR). Intergovernmental panel on climate change, Geneva; p 151

Iraqi Ministries of Environment (2006) Water resources, New Aden master plan for integrated water resources management in the marshlands area, Italy

Jain S, Panda J, Kant S (2014) Possible socio-scientific issues of land-use and land-cover change impact and associated tools of study with a special reference to Delhi-Mumbai Industrial Corridor Region. Int J Earth Atmos Sci 1:58–70

Jassim HM, Fakhri HI, Hayfaa AJ (2016) Environmental impact of electrical power generators in Iraq. Int J Eng Technol Manag Appl Sci 4:122–134

Kadhim AA, Shortridge A, Al-Nasrawi AKM (2021) Causes and consequences of environmental degradation along the Shatt Al–Arab River: a coupled human and natural systems (CHANS) perspective. GeoJournal 86:2709–2722

Karpouzos DK, Kavalieratou S, Babajimopoulos C (2010) Trend analysis of precipitation data in Pieria Region (Greece). Eur Water 30:30–40

Kotagama OW, Pathirage S, Perera K et al (2023) Modelling predictive changes of blue carbon due to sea-level rise using InVEST model in Chilaw Lagoon, Sri Lanka. Model Earth Syst Environ 9:585–599

Ladiray D, Quenneville B (2012) Seasonal adjustment with the X-11 method. Springer, Berlin

Lazaridis M (2011) First principles of meteorology. In: First principles of meteorology and air pollution. Environ Pollut. vol 19 Springer, Dordrecht

Li X, Chen H, Liao H et al (2017) Potential effects of land cover change on temperature extremes over Eurasia: current versus historical experiments. Int J Climatol 37:59–74

Malik MA, Dar AQ, Jain MK (2022) Modelling the influence of changing climate on the hydrology of high elevation catchments in NW Himalaya's. Model Earth Syst Environ 8:4487–4496

Mansouri Daneshvar MR, Ebrahimi M, Nejadsoleymani H (2019) An overview of climate change in Iran: facts and statistics. Environ Syst Res 8:1–10

Morison JIL, Baker NR, Mullineaux PM, Davies WJ (2008) Improving water use in crop production. Philos Trans R Soc B Biol Sci 363:639–658

Mousavi A, Ardalan A, Takian A et al (2020) Climate change and health in Iran: a narrative review. J Environ Heal Sci Eng 18:367–378

National Academies of Sciences (2020) Climate change: evidence and causes update 2020. Natl Acad Press Washington. https://doi.org/10.17226/25733

Niu G, Yang Z, Mitchell KE et al (2011) The community Noah land surface model with multiparameterization options (Noah-MP): 1. Model description and evaluation with local-scale measurements. J Geophys Res Atmos 116. https://doi.org/10.1029/2010JD015139

Odnoletkova N, Patzek T, Howarth N (2020) Staying cool in a warming climate: Temperature, electricity and air conditioning in Saudi Arabia

Oke TR (1982) The energetic basis of the urban heat island. Q J R Meteorol Soc 108:1–24

Osman-Elasha B (2010) Mapping of Climate Change Threats and Human Development Impacts in the Arab Region. Research Papers Series, UNDP, 2008 Arab Human Development Report

Pachauri RK, Reisinger A (2008) Climate Change 2007: Synthesis Report (IPCC, Geneva, Switzerland)

Pachauri RK, Allen MR, Barros VR et al (2014) Climate change 2014: synthesis report. Contribution of Working Groups I, II and III to the fifth assessment report of the Intergovernmental Panel on Climate Change. Ipcc

Panda A, Sahu N (2019) Trend analysis of seasonal rainfall and temperature pattern in Kalahandi, Bolangir and Koraput districts of Odisha. India Atmos Sci Lett 20:e932

Parmesan C, Yohe G (2003) A globally coherent fingerprint of climate change impacts across natural systems. Nature 421:37–42

Partow H (2001) The Mesopotamian Marshlands: Demise of an Ecosystem," Division of Early Warning and Assessment, United Nations Environment Programme, UNEP Publication UNEP/DEWA/ TR.01-3. Nairobi (Kenya)

Partal T, Kahya E (2006) Trend analysis in Turkish precipitation data. Hydrol Process an Int J 20:2011–2026

Peres CA, Emilio T, Schietti J et al (2016) Dispersal limitation induces long-term biomass collapse in overhunted Amazonian forests. Proc Natl Acad Sci 113:892–897

Philander SG (2008) Encyclopedia of global warming and climate change: AE. Sage

Pohlert T (2016) Non-parametric trend tests and change-point detection. CC BY-ND 4:1–18

Poulopoulos SG, Inglezakis VJ (2016) Environment and development: basic principles, human activities, and environmental implications. Elsevier

Rago MM, Urretavizcaya MF, Defossé GE (2021) Relationships among forest structure, solar radiation, and plant community in ponderosa pine plantations in the Patagonian steppe. For Ecol Manage 502:119749

Rodell M, Velicogna I, Famiglietti JS (2009) Satellite-based estimates of groundwater depletion in India. Nature 460:999–1002

Roe GH, Steig EJ (2004) Characterization of millennial-scale climate variability. J Clim 17:1929–1944

Ru X, Song H, Xia H et al (2022) Effects of land use and land cover change on temperature in summer over the Yellow River Basin. China Remote Sens 14:4352

Sacks WJ, Cook BI, Buenning N et al (2009) Effects of global irrigation on the near-surface climate. Clim Dyn 33:159–175

Sang Y-F, Wang Z, Liu C (2014) Comparison of the MK test and EMD method for trend identification in hydrological time series. J Hydrol 510:293–298

Sen PK (1968) Estimates of the regression coefficient based on Kendall's tau. J Am Stat Assoc 63:1379–1389

Stocker T (2014) Climate change 2013: the physical science basis: Working Group I contribution to the Fifth assessment report of the Intergovernmental Panel on Climate Change. Cambridge university press, Cambridge

Tabari H, Talaee PH (2011) Analysis of trends in temperature data in arid and semi-arid regions of Iran. Glob Planet Change 79:1–10

Talagala TS, Hyndman RJ, Athanasopoulos G (2018) Meta-learning how to forecast time series. Monash Econometrics Bus Stat Working Pap 6(18):16

Tarawneh QY, Chowdhury S (2018) Trends of climate change in Saudi Arabia: implications on water resources. Climate 6:8

The World Bank (2022) World Bank Publications, The World Bank Group, 1818 H Street NW, Washington, DC 20433, USA

Theil H (1950) A rank-invariant method of linear and polynomial regression analysis. Indag Math 12:173

Thiery W, Davin EL, Lawrence DM et al (2017) Present-day irrigation mitigates heat extremes. J Geophys Res Atmos 122:1403–1422

Verbesselt J, Hyndman R, Newnham G, Culvenor D (2010) Detecting trend and seasonal changes in satellite image time series. Remote Sens Environ 114:106–115

Wille B (2019) Basra is thirsty: Iraq's failure to manage the water crisis, Human Rights Watch, New York, p 131

Wong CP, Jiang B, Bohn TJ et al (2017) Lake and wetland ecosystem services measuring water storage and local climate regulation. Water Resour Res 53:3197–3223

Xia L, Gao Y, Wang W et al (2014) Climate change and applicability of GLDAS in the headwater of the Yellow River Basin. Adv Earth Sci 29:531–540

Zhang Q, Peng J, Xu C-Y, Singh VP (2014) Spatiotemporal variations of precipitation regimes across Yangtze River Basin, China. Theor Appl Climatol 115:703–712

Zhang X, Vincent LA, Hogg WD, Niitsoo A (2000) Temperature and precipitation trends in Canada during the 20th century. Atmos Ocean 38:395–429